Acta Crystallographica Section F
Structural Biology and Crystallization Communications
ISSN 1744-3091

X-ray structure of the NO-bound Cu_B in bovine cytochrome *c* oxidase

Kazuhiro Ohta,[a] Kazumasa Muramoto,[b] Kyoko Shinzawa-Itoh,[b] Eiki Yamashita,[a] Shinya Yoshikawa[b]* and Tomitake Tsukihara[a,b]

[a]Institute for Protein Research, Osaka University, OLABB, 6-2-6 Furuedai, Suita, Osaka 565-0874, Japan, and [b]Department of Life Science, University of Hyogo, 3-2-1 Kouto, Kamigohri, Akoh, Hyogo 678-1297, Japan

Correspondence e-mail: yoshi@sci.u-hyogo.ac.jp

Received 15 December 2009
Accepted 22 December 2009

PDB Reference: bovine heart cytochrome *c* oxidase, 3abk.

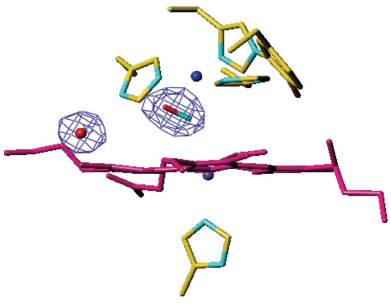

The X-ray crystallographic structure of nitric oxide-treated bovine heart cytochrome *c* oxidase (CcO) in the fully reduced state has been determined at 50 K under light illumination. In this structure, nitric oxide (NO) is bound to the CcO oxygen-reduction site, which consists of haem and a Cu atom (the haem a_3–Cu_B site). Electron density for the NO molecule was observed close to Cu_B. The refined structure indicates that NO is bound to Cu_B in a side-on manner.

1. Introduction

Cytochrome *c* oxidase (CcO) is the terminal oxidase of the respiratory chain and resides in the mitochondrial inner membrane or the bacterial cytoplasmic membrane (Ferguson-Miller & Babcock, 1996). CcO contains four redox-active metal sites: haem *a*, haem a_3, Cu_A and Cu_B. The haem a_3–Cu_B site in the transmembrane region catalyzes the reduction of molecular oxygen to two water molecules. Substrate O_2 is transferred to the haem a_3–Cu_B site through a hydrophobic channel in the transmembrane region. The electrons are transmitted from cytochrome *c* on the positive-side (exterior) surface of CcO through the Cu_A site and haem *a*. The protons are taken up from the negative-side (interior) region and are transferred through specific hydrogen-bond networks in the transmembrane region. In addition to the protons for water production, protons are transferred through CcO across the membrane, generating the proton electrochemical gradient.

Nitric oxide (NO), which is an excellent probe for the O_2-reduction site, inhibits the catalytic activity of CcO (Cooper & Brown, 2008; Brunori *et al.*, 2006). Previous spectroscopic studies have reported that NO binds to the haem a_3–Cu_B site in the reduced state (Brudvig *et al.*, 1980; Rousseau *et al.*, 1988). NO can be photodissociated from the haem a_3 iron (Fe_{a3}) and rebinds to Fe_{a3} in a temperature-dependent manner (Yoshida *et al.*, 1980; LoBrutto *et al.*, 1984). The rebinding rate of NO to Fe^{2+}_{a3} is negligibly slow at temperatures below 60 K.

In previous studies, we have determined the atomic structure of the haem a_3–Cu_B site of bovine heart CcO in both oxidized and reduced states and in complex with inhibitors (Yoshikawa *et al.*, 1998; Tsukihara *et al.*, 2003; Aoyama *et al.*, 2009). Of the four redox-active metal sites of CcO, the function of Cu_B is the least well understood, since no reliable spectroscopy is available for structural and functional studies of the Cu_B site. By analogy to the photodissociated CO derivative of CcO (Fiamingo *et al.*, 1982), binding of NO to Cu_B under light illumination is most likely. However, formation of the Cu_B–NO complex has not been demonstrated experimentally. In order to probe the Cu_B site with NO, we examined the X-ray structure of the NO adduct of bovine heart CcO under light illumination. Here, we report the NO-bound structure of bovine heart CcO in the fully reduced state at 50 K under light illumination.

2. Materials and methods

2.1. Preparation of crystals of the complex of bovine heart CcO with NO

CcO in the fully oxidized state was purified from bovine heart mitochondria and crystallized as described previously (Tsukihara *et*

Table 1
X-ray diffraction data and refinement statistics for NO-bound reduced CcO at 50 K under light illumination.

Diffraction data	
σ cutoff	−3
Resolution (Å)	75.6–2.00 (2.02–2.00)
Observed reflections	1946933 (61603)
Independent reflections	444573 (14713)
Averaged redundancy†	4.4 (4.2)
$\langle I/\sigma(I)\rangle$‡	18.6 (1.57)
Completeness§ (%)	98.9 (99.2)
$R_{\rm merge}$¶ (%)	10.4
Refinement	
Resolution (Å)	40.0–2.00 (2.03–2.00)
R†† (%)	18.3 (28.0)
$R_{\rm free}$‡‡ (%)	21.9 (34.0)
R.m.s.d.§§ bonds (Å)	0.032
R.m.s.d.§§ angles (°)	2.7

† Redundancy is the number of observed reflections for each independent reflection. ‡ $\langle I/\sigma(I)\rangle$ is the average of the intensity signal-to-noise ratio. § Completeness is the percentage of independent reflections observed. ¶ $R_{\rm merge} = \sum_{hkl}\sum_i |I_i(hkl) - \langle I(hkl)\rangle|/\sum_{hkl}\sum_i I_i(hkl)$, where $I_i(hkl)$ is the intensity value of the ith measurement of hkl and $\langle I(hkl)\rangle$ is the corresponding mean value of $I_i(hkl)$ for all i measurements. The summation is over reflections with $I/\sigma(I)$ larger than −3. †† R is the conventional crystallographic R factor, $R = \sum_{hkl}||F_{\rm obs}| - |F_{\rm calc}||/\sum_{hkl}|F_{\rm obs}|$, where $F_{\rm obs}$ and $F_{\rm calc}$ are the observed and calculated structure factors, respectively. ‡‡ $R_{\rm free}$ is the free R factor in the program *X-PLOR* (Brünger, 1992) evaluated for 5% of the reflections that were excluded from the refinement. §§ Root-mean-square deviation.

al., 1995). The oxidized crystals were stabilized at 277 K in 40 m*M* MES–Tris buffer pH 5.8 containing 0.2%(*w*/*v*) *n*-decyl β-D-maltoside and 1%(*w*/*v*) polyethylene glycol 4000 (Sigma). The CcO crystals were reduced with 5 m*M* sodium dithionite supplemented with 5 m*M* glucose, 1 µ*M* glucose oxidase and 0.5 µ*M* catalase as described previously (Tsukihara *et al.*, 2003). The NO-bound reduced enzyme was prepared by the addition of 5 m*M* sodium nitrite (Yonetani *et al.*, 1972; Brudvig *et al.*, 1980). Binding of NO to the fully reduced crystal was confirmed by measurement of the α-band absorption using a microspectrometer as described previously (Aoyama *et al.*, 2009). For the X-ray diffraction measurements, the crystals were frozen in a cryo-helium stream at 50 K in the presence of 45% ethylene glycol as a cryoprotectant and illuminated with a halogen lamp.

2.2. X-ray structure determination

X-ray diffraction intensity data were collected at a wavelength of 0.9 Å on BL44XU at SPring-8, Hyogo, Japan. Data processing and scaling were carried out using *DENZO* and *SCALEPACK* (Otwinowski & Minor, 1997). The structure amplitudes ($F_{\rm o}$) were calculated using the *CCP*4 program *TRUNCATE* (French & Wilson, 1978). The initial phases to 4 Å resolution were obtained by the

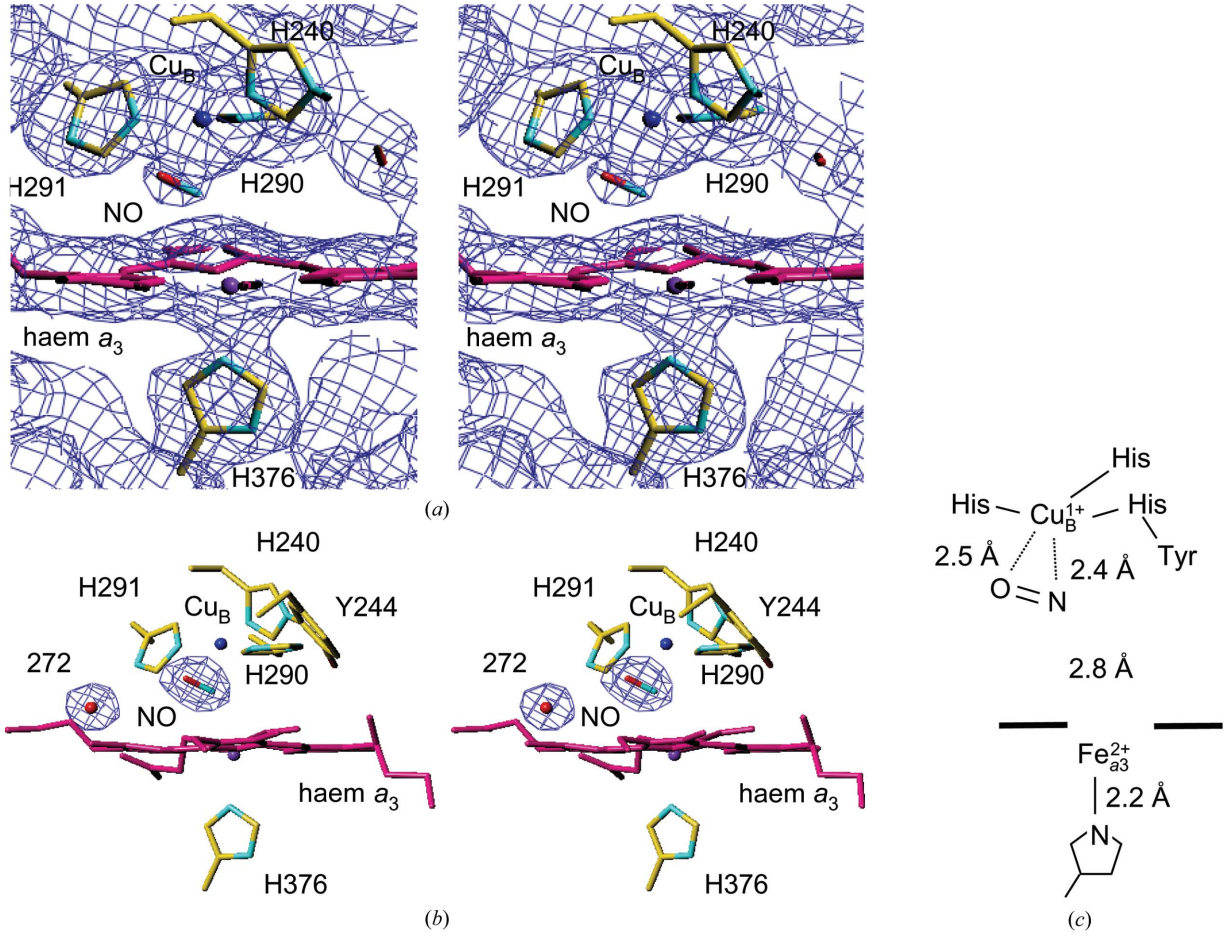

Figure 1
(*a*) Stereoview of the MR/DM electron-density map of the NO-bound reduced haem a_3–Cu_B sites. The electron density (blue cages) is contoured at the 1.2σ level. (*b*) Stereoview of the refined structure of the NO-bound reduced haem a_3–Cu_B sites. The ($F_{\rm o} - F_{\rm c}$) electron density (blue cages), in which NO and one water (wat272) were omitted from the $F_{\rm c}$ calculation, is contoured at the 5.8σ level. C, N and O atoms in the model structure are shown in yellow, blue and red, respectively. The figures were drawn using the program *TURBO-FRODO* (Jones, 1978). (*c*) Schematic representation of the haem a_3–Cu_B site. The distance between Fe_{a3} and Cu_B is 4.9 Å.

molecular-replacement (MR) method using the previously determined structure of the fully oxidized protein (Shinzawa-Itoh *et al.*, 2007; PDB code 2dyr) as a model. Phase extension to 2.0 Å resolution was carried out by density modification in conjunction with non-crystallographic symmetry averaging using the *CCP*4 program *DM* (Cowtan, 1994). The resultant phase angles ($\alpha_{MR/DM}$) were used to calculate the electron-density map (MR/DM map) with Fourier coefficients $F_o\exp(i\alpha_{MR/DM})$.

The atomic coordinates of fully reduced CcO (Muramoto *et al.*, 2007; PDB code 2eij) were used to build an initial model in the MR/DM map. Structural refinement was carried out using the program *X-PLOR* (Brünger *et al.*, 1987) and the *CCP*4 program *REFMAC*5 (Murshudov *et al.*, 1997). Bulk-solvent correction, anisotropic scaling of the observed and calculated structure amplitudes and TLS parameters were incorporated into the refinement calculation. The individual anisotropic *B* factor was refined for all the Fe and Cu atoms. During the refinement, the N—O bond length was fixed at 1.15 Å, but the Fe_{a3}—N, Fe_{a3}—O, Cu_B—N and Cu_B—O distances and the Fe_{a3}—N—O, O—N—Cu_B and N—O—Cu_B angles were not geometrically restrained. The progress of the refinement was assessed by a decrease in the *R* and R_{free} values (Brünger, 1992) calculated at each step of the refinement. The correct geometry of the refined structure of NO was confirmed by visual inspection of the electron density observed in $(F_o - F_c)\exp(i\alpha_c)$ difference Fourier electron-density maps, where F_c and α_c are the structure amplitudes and phase angles, respectively, calculated from the refined model excluding NO.

3. Results and discussion

3.1. Structure of the NO-bound Cu_B in bovine CcO

The X-ray diffraction data set for fully reduced CcO complexed with NO was collected at 50 K under light illumination. Statistics for the data set at 2.0 Å resolution are summarized in Table 1. The MR/DM electron-density map calculated as described in §2 clearly revealed electron density around the haem a_3–Cu_B site (Fig. 1*a*). The electron-density hump between Cu_B and Fe_{a3} is assignable as the NO molecule because no electron density is observed in the fully reduced CcO structure (Yoshikawa *et al.*, 1998). The electron density of NO is close to Cu_B, which indicates that NO interacts with Cu_B rather than with Fe_{a3}.

The NO molecule was incorporated into the electron density and refinement was continued. The Fe_{a3}—NO and Cu_B—NO bond distances were not restrained in the course of the refinement. The refined structure showed that the Fe_{a3}—N distance (2.8 Å) was significantly longer than the Cu_B—N (2.4 Å) and Cu_B—O (2.5 Å) distances (Figs. 1*b* and 1*c*) and that NO bound to Cu_B in a side-on binding mode without coordination to Fe_{a3}. An alternative refinement was performed to confirm the side-on binding. An initial structure of NO bound to Cu_B in an end-on mode was converted to the side-on binding to Cu_B by the refinement. The refined temperature factors of the N and O atoms in NO and Fe_{a3} and Cu_B were 32, 36, 27 and 29 $Å^2$, respectively, indicating that temperature factor of NO is slightly higher than those of the surrounding molecules or that the occupancy of NO is not full. Since an alternative structure in which the two atoms of NO are mutually exchanged cannot be excluded in the present crystal structure determination, the assignment of the N and O atoms is arbitrary.

Based on spectroscopic data from previous studies, NO is bound to the reduced Fe_{a3} in the haem a_3–Cu_B site (Brudvig *et al.*, 1980; Rousseau *et al.*, 1988). The treatment of CcO crystals with dithionite and nitrite in this study must provide an Fe_{a3} site that is saturated with NO, as confirmed by absorption spectroscopic analysis of the crystal. Previous reports (Yoshida *et al.*, 1980; LoBrutto *et al.*, 1984) strongly suggested that under the present conditions (illumination with a halogen lamp at 50 K) NO is photodissociated from Fe_{a3} and rebinding to Fe_{a3} is negligible. Therefore, the observed geometry of NO in this study indicates that the photodissociated form of NO stabilizes the nearby Cu_B in a side-on binding. It should be noted that no direct experimental evidence has been reported for NO binding to Cu_B. Three histidine imidazoles serve as the Cu_B ligands. Therefore, NO is stabilized at the fourth coordination position of Cu_B, where no ligand is located in the fully reduced state of CcO, although the space is wide enough for binding of a diatomic ligand (Figs. 1*b* and 1*c*). This structure, together with the geometry of NO at Cu_B^{1+} showing a weak side-on binding, strongly suggests that Cu_B controls O_2 supply to Fe_{a3}^{2+} by reversibly trapping O_2 without forming the peroxide intermediate.

References

Aoyama, H., Muramoto, K., Shinzawa-Itoh, K., Hirata, K., Yamashita, E., Tsukihara, T., Ogura, T. & Yoshikawa, S. (2009). *Proc. Natl Acad. Sci. USA*, **106**, 2165–2169.

Brudvig, G. W., Stevens, T. H. & Chan, S. I. (1980). *Biochemistry*, **19**, 5275–5285.

Brünger, A. T. (1992). *Nature (London)*, **355**, 472.

Brünger, A., Kuriyan, J. & Karplus, M. (1987). *Science*, **235**, 458–460.

Brunori, M., Forte, E., Arese, M., Mastronicola, D., Giuffrè, A. & Sarti, P. (2006). *Biochim. Biophys. Acta*, **1757**, 1144–1154.

Cooper, C. E. & Brown, G. C. (2008). *J. Bioenerg. Biomembr.* **40**, 533–539.

Cowtan, K. (1994). *Jnt CCP4/ESF–EACBM Newsl. Protein Crystallogr.* **31**, 34–38.

Ferguson-Miller, S. & Babcock, G. T. (1996). *Chem. Rev.* **96**, 2889–2907.

Fiamingo, F. G., Altshuld, R. A., Moh, P. P. & Alben, J. O. (1982). *J. Biol. Chem.* **257**, 1639–1650.

French, S. & Wilson, K. (1978). *Acta Cryst.* A**34**, 517–525.

Jones, T. A. (1978). *J. Appl. Cryst.* **11**, 268–272.

LoBrutto, R., Wei, Y.-H., Yoshida, S., Van Camp, H. L., Scholes, C. P. & King, T. E. (1984). *Biophys. J.* **45**, 473–479.

Muramoto, K., Hirata, K., Shinzawa-Itoh, K., Yoko-o, S., Yamashita, E., Aoyama, H., Tsukihara, T. & Yoshikawa, S. (2007). *Proc. Natl Acad. Sci. USA*, **104**, 7881–7886.

Murshudov, G. N., Vagin, A. A. & Dodson, E. J. (1997). *Acta Cryst.* D**53**, 240–255.

Otwinowski, Z. & Minor, W. (1997). *Methods Enzymol.* **276**, 307–326.

Rousseau, D. L., Singh, S., Ching, Y. & Sassaroli, M. (1988). *J. Biol. Chem.* **263**, 5681–5685.

Shinzawa-Itoh, K., Aoyama, H., Muramoto, K., Terada, H., Kurauchi, T., Tadehara, Y., Yamasaki, A., Sugimura, T., Kurono, S., Tsujimoto, K., Mizushima, T., Yamashita, E., Tsukihara, T. & Yoshikawa, S. (2007). *EMBO J.* **26**, 1713–1725.

Tsukihara, T., Aoyama, H., Yamashita, E., Tomizaki, T., Yamaguchi, H., Shinzawa-Itoh, K., Nakashima, R., Yaono, R. & Yoshikawa, S. (1995). *Science*, **269**, 1069–1074.

Tsukihara, T., Shimokata, K., Katayama, Y., Shimada, S., Muramoto, K., Aoyama, H., Mochizuki, M., Shinzawa-Itoh, K., Yamashita, E., Yao, M., Ishimura, Y. & Yoshikawa, S. (2003). *Proc. Natl Acad. Sci. USA*, **100**, 15304–15309.

Yonetani, T., Yamamoto, H., Erman, J. E., Leigh, J. S. & Reed, G. H. (1972). *J. Biol. Chem.* **247**, 2447–2455.

Yoshida, S., Hori, H. & Orii, Y. (1980). *J. Biochem.* **88**, 1623–1627.

Yoshikawa, S., Itoh-Shinzawa, K., Nakashima, R., Yaono, R., Yamashita, E., Inoue, N., Yao, M., Fei, M. J., Libeu, C. P., Mizushima, T., Yamaguchi, H., Tomizaki, T. & Tsukihara, T. (1998). *Science*, **280**, 1723–1729.